Effects of crosslinking on the physical solid-state and dissolution properties of 3D-printed theophylline tablets

Anderspuk, Hele

2021-12

Anderspuk , H , Viidik , L , Olado , K , Kogermann , K , Juppo , A , Heinämäki , J & Laidmäe , I 2021 , ' Effects of crosslinking on the physical solid-state and dissolution properties of 3D-printed theophylline tablets ' , Annals of 3D Printed Medicine , vol. 4 , 100031 . https://doi.org/10.1016/j.stlm.2021

http://hdl.handle.net/10138/341470
https://doi.org/10.1016/j.stlm.2021.100031

Annals of 3D Printed Medicine 4 (2021) 100031

Contents lists available at ScienceDirect

Annals of 3D Printed Medicine

journal homepage: www.elsevier.com

Research paper

Effects of crosslinking on the physical solid-state and dissolution properties of 3D-printed theophylline tablets

Hele Anderspuk[a,b,1], Laura Viidik[a,1,*], Kristjan Olado[a], Karin Kogermann[a], Anne Juppo[b], Jyrki Heinämäki[a], Ivo Laidmäe[a,c]

[a] Institute of Pharmacy, Faculty of Medicine, University of Tartu, Nooruse Str. 1, 50411 Tartu, Estonia
[b] Division of Pharmaceutical Chemistry and Technology, Faculty of Pharmacy, Viikinkaari 5E, 00014 University of Helsinki, Finland
[c] Department of Immunology, Institute of Biomedicine and Translational Medicine, Faculty of Medicine, University of Tartu, Ravila Str. 19, 50411 Tartu, Estonia

ARTICLE INFO

Article History:
Received 16 June 2021
Revised 16 August 2021
Accepted 22 September 2021
Available online 24 September 2021

Keywords:
3D-printing
UV-crosslinking
Gamma-radiation crosslinking
Drug release
Polyethylene oxide
Theophylline

ABSTRACT

Crosslinking is an established treatment to alter the physicochemical and functional properties of polymers through the creation of bonds between the polymer chains. Polymers can be crosslinked via radiation in the presence of photo-initiator. The aim of the present study was to formulate 3D-printed theophylline (THEO) tablets using polyethylene oxide (PEO) as a carrier polymer, and to study the influence of crosslinking on the drug release behavior. The tablets were 3D-printed using the aqueous solution of PEO and THEO (80:20 w/w) with a micro-extrusion-based printing setup. A photo-initiator (4-hydroxybenzophenone) was added into the printing solutions, and the injectability of the solutions was investigated prior to printing. The 3D-printed tablets were crosslinked after printing using ultraviolet (UV) or gamma-radiation, and crosslinking was verified by means of Fourier-transform infrared (FTIR) spectroscopy. The maximum injection force of aqueous printing solutions of PEO and THEO was close to that observed with the pure PEO solution. Increasing the number of printing layers in the 3D-printed tablets resulted in a slower drug release *in vitro*. Gamma-radiation in a nitrogen environment and UV-crosslinking made the carrier polymer (PEO) less water-soluble, but such crosslinking did not affect the release rate of the tablets. Surprisingly, even faster drug release behavior was found with the crosslinked 3D-printed tablets compared to that of non-crosslinked tablets. More research work is needed on the impact of 3D-printed tablet layering thickness and crosslinking for tailoring drug release behavior.

1. Introduction

Three-dimensional (3D) printing is an additive manufacturing technology enabling the layer-by-layer creation of a pre-designed 3D object. Today, 3D printing methods have found multiple uses also in pharmaceutical sciences [1–3]. Nozzle-based 3D-printing systems are applicable for printing polymeric semisolid materials. Such systems use a computer-controlled production technique where semi-solid materials are deposited layer-by-layer through a nozzle to obtain the final product in a desired 3D structure [4]. The nozzle (alternatively the platorm) is moving in three different directions (x, y and z dimensions) to form the desired shape. Such 3D-printing methods require the continous extrusion of the printing material from a syringe-like printing head at specific speed and pressure [5].

There are many advantages associated with the use of nozzle-based 3D printing technologies. Printing time is shorter due to a decreased number of process steps needed, and printing yields low waste of materials [6]. Furthermore, heating is not required [5], thus making it a suitable method for thermolabile active pharmaceutical ingredients (APIs) [7]. A drying step, however, is needed as a post-printing phase since the printed formulations contain solvents, and this could result in product deformation [4,8]. Semi-solid printing mixtures mostly consist of a suitable polymer, solvent and other excipients with the material properties advancing 3D printing [2]. In the 3D printing formulation, the most important excipient is the carrier polymer determining the formation and performance of the final product [4]. Hydrogels and natural polymers are often used in nozzle-based 3D printing [9,10].

Rheological properties such as viscosity and viscoelasticity are important material-related factors affecting the 3D printing of liquid and semisolid materials [4,11]. If the viscosity of a printing liquid or semisolid is too high, the risk for a nozzle blockage is increased. On the other hand, if the viscosity is too low, a desired 3D structure is

* Corresponding author at: University of Tartu, Faculty of Medicine, Institute of Pharmacy, Nooruse Str. 1, 50411 Tartu, Estonia.
E-mail address: laura.viidik@ut.ee (L. Viidik).
[1] Contributed equally to this work.

https://doi.org/10.1016/j.stlm.2021.100031

not possible to be established. Thixotropic or shear-thinning behavior of a printing liquid (or semisolid) is beneficial for enhancing material flow through a nozzle system, and yet forming a stable structure after being deposited onto the printing plate. Therefore, the type and concentration of polymer, and the amount of solvent are the critical material-related factors in 3D printing of novel drug delivery systems (DDSs) [12].

Hydrogels are widely used as biocompatible materials in various medical applications [9,13]. Hydrogels loaded with various therapeutic agents enable to formulate oral prolonged-release DDSs, which have many advantages over *e.g.*, conventional immediate-release dosage forms. Hydrogels prepared by photo-crosslinking can also be used as a permissive bioresorbable carrier system for both hydrophilic and hydrophobic drugs [10,14]. The properties and performance of such hydrogels can be tailored for the specific pharmaceutical applications by using a suitable crosslinking agent [15]. The hydrogels applied in 3D printing are mostly crosslinked either before or after a printing process. Recently, however, an increased interest is being shown on *in situ* layer-by-layer crosslinking [16–18], which has also been used in electrospinning [19,20].

Polyethylene oxide (PEO) is a hydrophilic semicrystalline synthetic polymer [21]. In our previous study, we investigated the 3D-printability of aqueous PEO gels [22]. PEO has also been used as a biocompatible material in medical 3D-printing applications [23,24]. PEO can be crosslinked via UV-radiation in the presence of photo-initiators, *e.g.* pentaerythritol tetra acrylate [25–27]. In addition, gamma-radiation has been used for crosslinking PEO [28–31]. Crosslinking, however, is known to alter many polymer properties. For example, the mechanical strength of the polymers and their resistance to high temperature, solvents and abrasion were shown to increase after crosslinking [32]. Crosslinking has also been applied for modifying the drug release and dissolution of oral DDSs [33].

The aim of this study was to design and characterize novel 3D-printed PEO-based tablets and to evaluate the effects of UV and gamma radiation-induced crosslinking on the *in- vitro* drug release behavior of tablets. Theophylline (THEO) was used as a model drug in 3D-printed tablets.

2. Materials and methods

2.1. Material preparation for printing solutions

Polyethylene oxide (PEO, Mw ~ 900 000, Sigma-Aldrich, USA) was used as a base polymer and anhydrous THEO (Sigma-Aldrich, Switzerland) as a model API at a w/w ratio of 80:20. THEO (0.375 g) was dissolved in 15 ml of distilled water and heated until fully dissolved. Then, 1.5 g of PEO was mixed into the solution. This printing solution was held overnight in a closed vessel for completing the dissolution of PEO. The photo-initiator, 4-hydroxybenzophenone (HBP, Sigma-Aldrich, USA) was mixed in a powder form (2.5% w/w of PEO used) into the solution prior to 3D-printing. For injectability studies, the two reference solutions (PEO_15 and PEO_10) were additionally prepared by dissolving 2.25 g and 1.5 g of PEO in 15 ml of distilled water, respectively.

2.2. Injectability

Brookfield CT3 Texture Analyzer (Middleboro, MA, USA) together with TexturePro CT software (AMETEK Brookfield, Middleboro, MA, USA) was used for measuring the injection force needed for pushing the printing solutions through a 21 G needle. The final printing solution (PEO and THEO 80:20) and reference solutions (PEO_15 and PEO_10) were tested. A 3-ml Luer lock Norm-Ject® syringe was filled and fixed at 2 ml of polymer solution. The syringe was securely placed between the fixtures of the texture analyzer, and a continuous speed of 1.0 mm/s was used for material extrusion from the syringe. All measurements were made in triplicate at room temperature (22 ± 2 °C).

2.3. 3D-printing

The cylindric model tablets were prepared using a micro-extrusion-based 3D printer (System 30 M, Hyrel 3D, USA) equipped with a KRA-15 extrusion head and a 21 G needle as a printing head nozzle. The printing head speed was set at 0.5 mm/s and the printing plate temperature was 50 °C. Nine tablets were printed in one batch, and the number of material layers (*i.e.*, tablet thickness, referring to the batches as TH or TK) was varied in different batches. The tablet thickness was considered further on only *in vitro* drug release testing. The tablets were kept in a desiccator in a refrigerator (2–8 °C) before crosslinking and subsequent dissolution tests.

2.4. Crosslinking

The 3D-printed tablets were crosslinked using an UV transilluminator (GVM-20, 230 V, 50 Hz, 100 W, 2A, ⌀5 × 20, Serial 964215, Syngene, UK). The irradiation time was 15 min for the both sides of tablets (30 min in total for one tablet). These tablets are further referred to as TH_UV30 and TK_UV30. Potential swelling or the degradation of the 3D-printed solids were evaluated visually. Gamma-radiation induced crosslinking was carried out in Scandinavian Clinics Estonia OÜ, Alliku, Estonia. The measured radiation doses absorbed ranged from 31.3 kGy to 32.9 kGy. The tablets were gamma-radiated in an ambient air (TK_gamma) or in a nitrogen gas (TK_gammaN) to investigate the impact of environment during irradiation on the 3D-printed tablets.

2.5. Fourier-transform infrared spectroscopy

To evaluate the possible solid-state changes during 3D-printing process and crosslinking, the Fourier-transform infrared (FTIR) spectra of the pure components, physical mixtures (PM) and 3D-printed tablets were collected using an IRPrestige-21 spectrophotometer (Shimadzu Corp., Japan) and Specac Golden Gate Single Reflection attenuated total reflection crystal (Specac Ltd., UK). The analytical range used was from 600 cm^{-1} to 4000 cm^{-1}. All measurements were carried out in triplicate. The FTIR spectra were normalized and scaled.

2.6. Near-infrared spectroscopy

To study the drying of 3D-printed DDSs, near-infrared (NIR) spectra were measured with a AvaSpec-NIR256–2.2 spectrometer (Avantes, The Netherlands) equipped with a 256-pixel GaAs detector and tungsten halogen lamp (AvaLight-HAL). The NIR spectra were collected on the pure materials, PMs (freshly prepared and stored at 40 °C and 75% RH, and a drop of water added on the top of mixture) and 3D-printed tablets (FRESH, the tablet immediately after 3D-printing, and AGED, the tablet stored for a week in a desiccator in a refrigerator at 2–8 °C). All measurements were carried out in triplicate.

2.7. Differential scanning calorimetry

The thermal analysis was performed using a PerkinElmer DSC 4000 Differential Scanning Calorimeter (PerkinElmer, Inc, Waltham, MA, USA) to determine the melting temperature (T_m) for pure materials (THEO and PEO), PMs and 3D-printed multilayered tablets. The samples (4 mg) were prepared in sealed aluminum standard pans and an empty pan was used as a reference. The samples were heated (10 °C/min) from 20 °C to 300 °C under a nitrogen gas purge at the flow rate of 20 ml/min. The data were analyzed using Pyris software

Table 2
Visual appearance, weight and water uptake of 3D-printed tablets (n = 3). Key: TH = thin (tablet), TK = thick (tablet), TH_UV = thin UV-crosslinked 3D-printed tablets, TK_UV = thick UV-crosslinked 3D-printed tablets, TH_gamma = thin gamma-radiation crosslinked 3D-printed tablets.

Batch code	Visual appearance	Weight (mg)			Water uptake (%)
		Post-print	Pre-dissolution	Post-dissolution	
TH	white, dissolves in water	35 ± 5	34 ± 4	N/A	N/A
TH_UV	yellowish, fully gel-like when in water	37 ± 5	35 ± 4	184 ± 4	526%
TK	white, dissolves in water	71 ± 8	71 ± 8	N/A	N/A
TK_UV	yellowish, fully gel-like when in water	63 ± 5	63 ± 5	385 ± 35	611%
TK_gamma	white, dissolves in water	103 ± 4	91 ± 1	N/A	N/A

(PerkinElmer, Inc, Waltham, MA, USA). All measurements were performed in triplicate.

2.8. *Drug release* in vitro

The *in-vitro* dissolution tests were performed using a dissolution apparatus (Sotax AT7 Smart, Sotax, Switzerland) and a paddle method. A paddle speed was set at 50 rpm. The dissolution medium used was 500 ml of distilled water at 37 °C. The samples were assayed by UV spectrophotometry (Specord 200 plus, Analytik Jena, Germany) and compared to the theoretical drug content of these tablets. Dissolution tests were carried out in three parallels. The residual samples were weighed after the test, if possible. Water uptake (%) was calculated from the weight gain of these samples. The water-solubility behavior of batch TK_UV tablets were visually compared with round-shaped solvent cast UV-crosslinked free films of equivalent composition, diameter, and thickness.

2.9. *Data analysis*

Principal component analysis (PCA, Simca-*P*+ Version 12.0.1.0, Umetrics AB, Sweden) was applied for NIR spectra to evaluate the drying phenomena and process. Spectral range from 1200 to 2250 nm was used for multivariate data analysis. Standard Normal Variate (SNV) and the 1st derivative spectral pre-processing was performed. For the PCA model, the first three principal components (PC) were used to explain the data. The scores plot and loadings plot are shown where the scores reveal the spectral variation, and the loadings represent the spectral contribution to each PC.

A two-tailed unpaired *t*-test (MS Excel) was used to study the statistical difference between the groups. The results are given in average value of three measurements ± standard deviation (SD), if not otherwise stated.

3. Results and discussion

3.1. *Characterization of printing materials and 3D-printed tablets*

In the present study, we used the injectability method to investigate the effects of drug-loaded semisolids and their rheological properties on a 3D-printing process. Table 1 shows the maximum injection force values for the aqueous PEO gel and drug-loaded PEO gel samples in the injectability test. The maximum injection force for the aqueous PEO_10 and PEO_THEO solutions was 43.7 ± 6.2 N and 52.9 ± 2.2 N, respectively. The maximum forces of these two printing solutions were not statistically different (p = 0.057). A slight increase in the maximum force with the PEO-THEO solution is obviously due to the higher concentration of solids in the mixture. The PEO_15 solution was found more challenging to load into the syringe due to higher viscosity of the solution. In the injectability test, the PEO_15 solution presented also the highest maximum force value of 95.7 ± 5.9 N. The difference to the force values obtained with PEO_10 and PEO_THEO solutions was statistically significant ($p < 0.05$).

Table 1
Injectability of printing solutions (n = 3). Key: THEO = theophylline, PEO = polyethylene oxide.

Printing solution	Maximum injection force (N)
PEO_15	95.7 ± 5.9
PEO_10	43.7 ± 6.2
PEO_THEO	52.9 ± 2.2

The injectability test is widely used for determining the critical rheology-related parameters affecting the subcutaneous and intramuscular injection of APIs [34]. To date, this test method has not been used frequently in the evaluation of 3D printing materials, even though the test setup mimics well the syringe-like printing head of a nozzle-based 3D-printing system. Moreover, the test method enables visual monitoring of the flowing behavior of a printing solution and the formation or presence of air bubbles in the solution, thus predicting the success of a printing process.

With the aqueous solutions of PEO, the impact of the polymer concentration on the injection force is evident, and this finding is in good agreement with our previous studies on the effects of viscosity on 3D printing [22]. The high molecular weight of PEO can also play an important role in resisting injectability [35]. Despite of the adavantages of using an injectability test for predicting the materials behavior in 3D printing, there are some limitations related to this test. Such limitations include *e.g.*, the difference in the flow velocity of materials in the injectability test and extrusion-based 3D printing. Therefore, for improving the prediction capacity, it would be important to use the same shear rate levels in an injectability test as in the real extrusion-based 3D printing process.

Two batches of tablets varying with the number of layers were successfully 3D-printed. The physical appearance, weight and water uptake of the 3D-printed multilayered tablets are summarized in Table 2. The weight variation of the tablets was found to increase as the weight of the tablets was increased. This is most likely due to the uneven material deposition onto the tablets because of an increased printing time of the tablets with a higher number of layers. The printed tablets were white to off-white in color, and occasional lines of a material deposition can be discovered on the top surface of the tablets. UV-crosslinked tablets were the only one having a subtle yellowish tint. No visual deformation was observed on the surface of the UV-crosslinked tablets.

3.2. *Solid-state properties*

3.2.1. *Fourier-transform infrared spectroscopy*

FTIR spectroscopy was used to evaluate possible molecular interactions during a 3D-printing process and to confirm the crosslinking of PEO. Fig. 1 shows the FTIR spectra of pure materials, PMs and non-crosslinked 3D-printed tablets. PEO has characteristic peaks at 840 cm^{-1} (relates to bonds of CH_2), 1093 cm^{-1} (shows triplet C—O-C stretching [36]) and 2875 cm^{-1} (relates to C—H

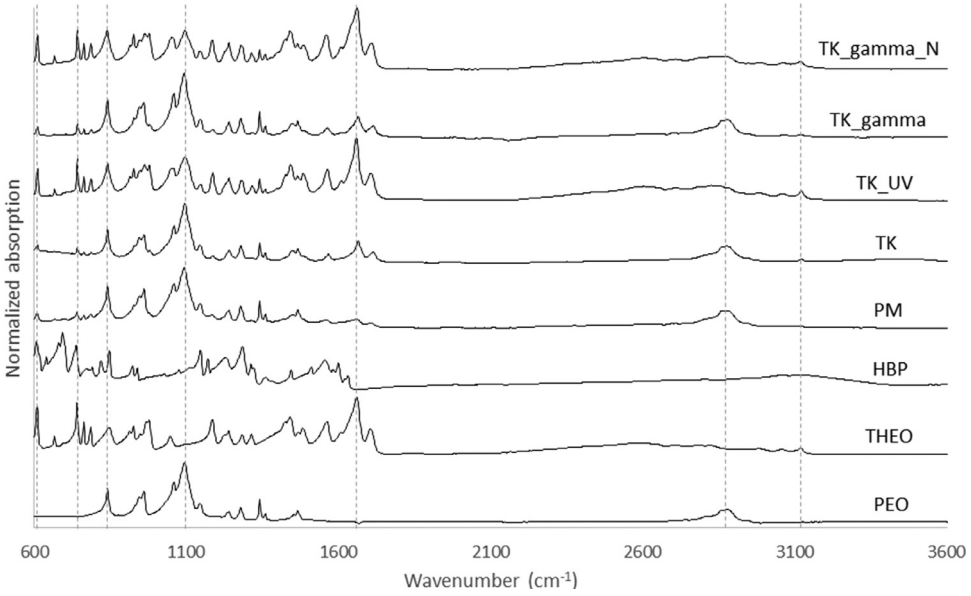

Fig. 1. Fourier-transform infrared (FTIR) spectra of (A) pure substances, physical mixture (PM) and 3D-printed non-crosslinked tablets, and (B) non-crosslinked, UV- and gamma-radiated crosslinked 3D-printed tablets. Key: THEO = theophylline, PEO = polyethylene oxide, HBP = 4-hydroxybenzophenone, TK = thick, *N* = nitrogen.

methylene stretching and shows semi-crystalline phase of PEO) [31]. All the abovementionted peaks are also seen in Fig. 1 for the PM and non-crosslinked 3D printed tablets at very similar intensity. The peaks for HBP were not detected in the abovementioned spectra. The specific absorption bands at 1658 cm^{-1} (related to C—O stretching for carbonyl group [37]) and at 3118 cm^{-1} (N–H stretching [38]) are characteristic for THEO. The barely visible absorption band at 1658 cm^{-1} can be seen in the FTIR spectra of PM and non-crosslinked 3D-printed tablets, being more intense in the latter. The phenomenon of lower intensity of the 1658 nm peak has been also reported in previous studies [39]. We found that similar behavior also applied for non-crosslinked tablets. Another characteristic peak for THEO is hardly seen at 3118 cm^{-1} in the FTIR-spectrum of the PM, but this peak is detectable in the FTIR-spectrum of the non-crosslinked tablets.

The efficacy and effects of the two radiation based crosslinking treatments on the solid-state properties of 3D-printed tablets were also compared. As seen in Fig. 1, the peaks displayed at 1093 cm^{-1} and at 2875 cm^{-1} in the FTIR-spectrum of the unradiated and gamma-radiated tablets correspond to the peaks characteristic for pure PEO. The specific peaks displayed in the FTIR spectra of the 3D-printed tablets irradiated by UV and gamma-radiation in a nitrogen environment showed very low intensity at 2875 cm^{-1} and the peaks at 1093 cm^{-1} nearly disappeared. This peak disappearance at 2875 cm^{-1} suggests molecular interactions by homolytic scission of C—H bonds (especially at the presence of nitrogen) as a crosslinking effect [40,41]. The intensity of 1658 cm^{-1} peak and the specific peak at 609 cm^{-1} and at 742 cm^{-1} of THEO are strongly distinguishable for the UV and gamma-radiation in nitrogen environment printed tablets compared to the gamma-radiated (without nitrogen) and non-crosslinked tablets. The characteristic high-intensity absorption peaks of THEO at 1658 cm^{-1}, 609 cm^{-1} and 742 cm^{-1} seen in the FTIR-spectra of UV- and gamma-radiated (nitrogen) tablets most likely indicate the presence of API in a free state. We can conclude that the presence of HBP as a photoinitiator and both UV- and gamma-radiation treatments (only in a nitrogen environment) result in successful crosslinking. In the literature, the use of nitrogen environment and/or antioxidants has been shown to benefit a crosslinking process and to prevent the chemical degradation of the polymer when gamma-radiation is used [31,42].

3.2.2. *Differential scanning calorimetry*

The thermal behavior of pure THEO and PEO, the PM, and non-crosslinked and UV-crosslinked 3D-printed tablets are presented in Fig. 2. The characteristic melting peaks for THEO and PEO are seen at 273 °C and at approximately 70 °C, respectively. With the non-crosslinked tablets the melting endotherm for PEO is displayed at a slightly lower temperature at 68 °C. As seen in Fig. 2, no melting endotherm of anhydrous THEO is displayed in the DSC thermograms of the PM and 3D-printed tablets. This is a well-known effect occuring with API-polymer mixtures where the polymer melts at a lower temperature than the melting temperature of API. This kind of behavior and phenomenon affect also the dissolution of THEO in PEO [39]. It is evident that THEO acting as a nucleating agent is able to facilitate the crystallization of polymer (PEO) [43]. The glass transition temperature of PEO was unobtainable under these testing conditions by DSC. We assume that no thermal degradation took place during a heating phase as there are no additional peaks seen in the DSC thermograms (Fig. 2).

3.2.3. *Near-infrared spectroscopy*

The importance of a drying step in the extrusion-based 3D printing of semisolid materials has been discussed previously in this paper. The water activity of 3D-printed tablets can be very high immediately after printing [44]. We compared the water content of the freshly prepared PMs, the PMs stored at high humidity conditions (40 °C/75% RH), and the freshly prepared and aged 3D-printed tablets (Fig. 3) by using NIR spectroscopy. NIR spectroscopy has been widely used for monitoring the drying as it is very sensitive towards H-bonding related with water molecules and it is easy to correlate the water content with NIR spectral features using modeling. No quantitative spectral analyses were performed, but the interpretation of the raw NIR spectra and PCA were used to qualitatively analyze the data and understand the drying effect. Fig. 3B shows the score plots of the PCA displaying two or three distinct groups for the NIR spectra. It was confirmed by the loadings plot that the present groups obtained in the PCA differ from each other based on the water content in the sample (Fig. 3C). The NIR spectra of the freshly prepared and stored 3D-printed tablets are grouped together with the NIR spectra of the freshly prepared PMs. The results suggest that the selected drying

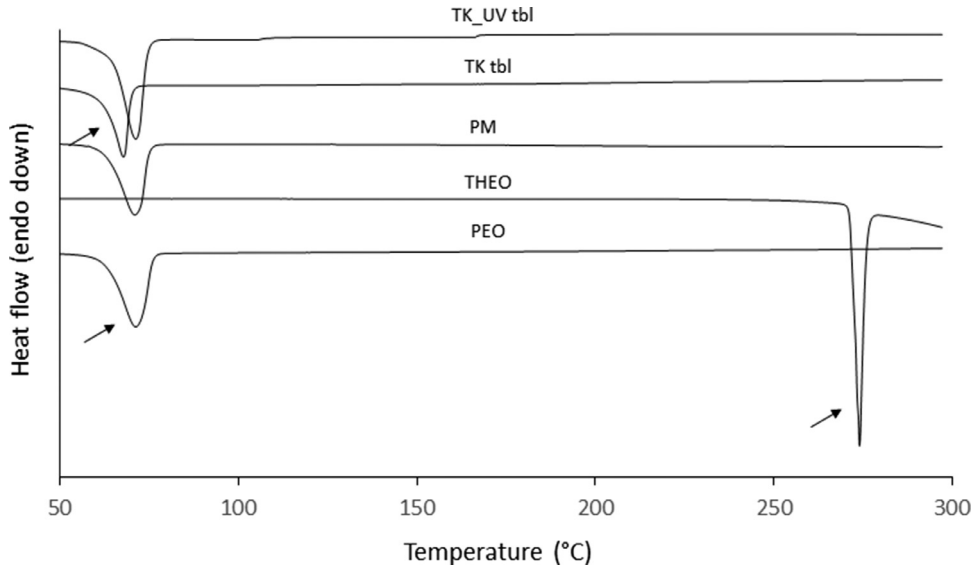

Fig. 2. Differential scanning calorimetry (DSC) thermograms of pure substances, physical mixture (PM), and non-crosslinked and UV-crosslinked 3D-printed tablet. Key: THEO = theophylline, PEO = polyethylene oxide, TK = thick.

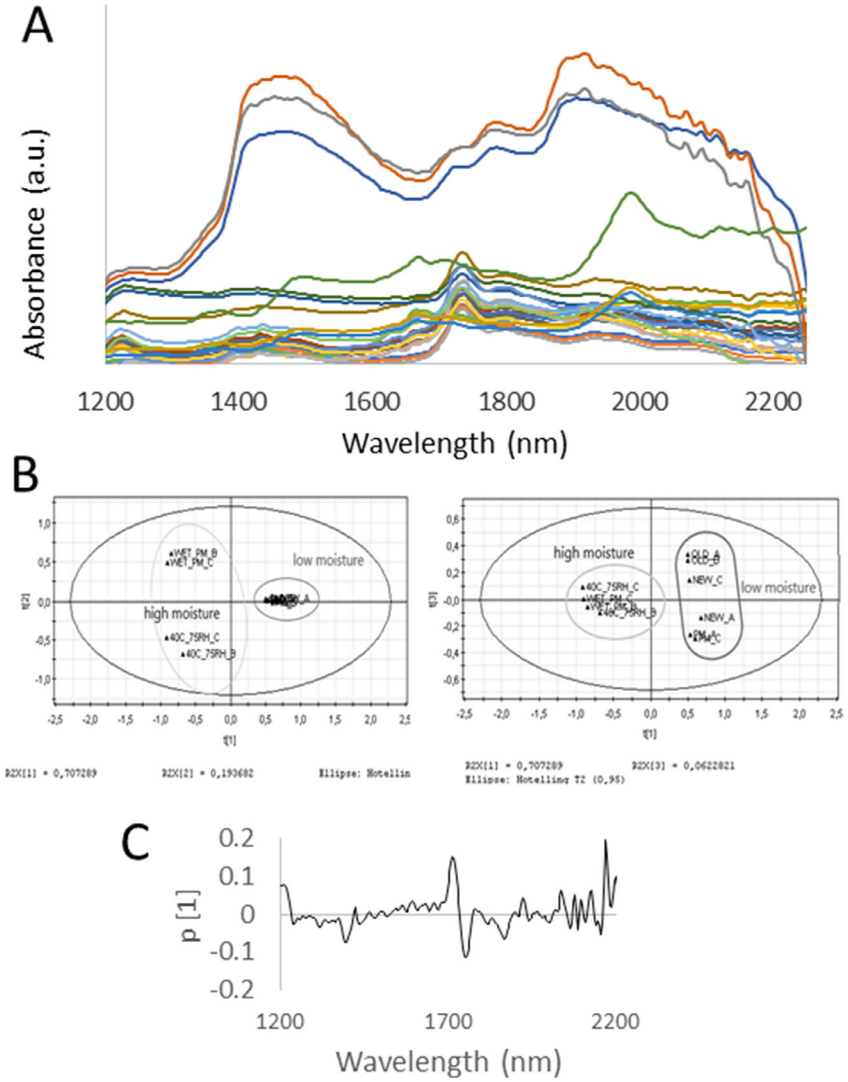

Fig. 3. Principal component analysis (PCA) of the water content of the freshly prepared physical mixtures (PMs), the PMs stored at high humidity conditions (40 °C/75% RH), and the freshly prepared and aged 3D-printed tablets. Fig. 3A: The untreated near-infrared (NIR) spectra of samples. Fig. 3B: The scores plot of t1/t2 and t1/t3. Fig. 3C: The loadings of principal component (PC) 1.

period for the 3D-printed tablets of the present size and shape is sufficient to remove any excess water.

The PCA model revealed that the largest differences between the samples were due to the presence of water. Hence, the first principal component (PC1) can be used to explain the water content in the samples, and it represented 70.1% of the spectral variation. As the PC1 loadings at the selected wavelengths were plotted, we found that the major differences in the variables occur at approximately 1200 nm, 1700 nm, 1750 nm, and 2170 nm. These differences can be associated with water absorption, since the bands at 1200 nm and 1700 nm correspond to the first and second overtone of the C—H stretching, and the band at 2200 nm corresponds to O—H stretch [45,46]. We observed also in our preliminary tests (data not shown) that the time required for the weight stabilization was longer with the thicker 3D-printed tablets than that with the corresponding thinner tablets. Therefore, the water content (NIR spectra) of the 3D-printed tablets needs to be evaluated (collected) over the time-period long enough to ensure the drying of such tablet preparations.

3.5. *Drug release* in vitro

Fig. 4 shows the influence of the number of layers and UV- or gamma-radiation crosslinking on the drug release behavior of the 3D-printed tablets. The dissolution results were calculated as the drug release of an average-weighed tablet of the batch considering the weights of the individual tablets selected in the test (Table 1). The UV-crosslinked thin 3D-printed tablets (TH, tablet height, h = 2 mm) presented an immediate-release dissolution pattern releasing the drug approximately within 30 min (Fig. 4A). With the non-crosslinked and UV-crosslinked thick tablets (TK, h = 5 mm), however, the amount of THEO released within 30 min (and within subsequent 60 min) was only about 50% of the theoretical amount of drug (Fig. 4A). Both thin and thick UV-crosslinked tablets exhibited an identical immediate-release behavior *in vitro*. The non-crosslinked thick 3D-printed tablets presented a prolonged drug-release pattern *in vitro* with the release of approximately 60% of the theoretical amount of drug within 90 min. Based on the visual inspection, the

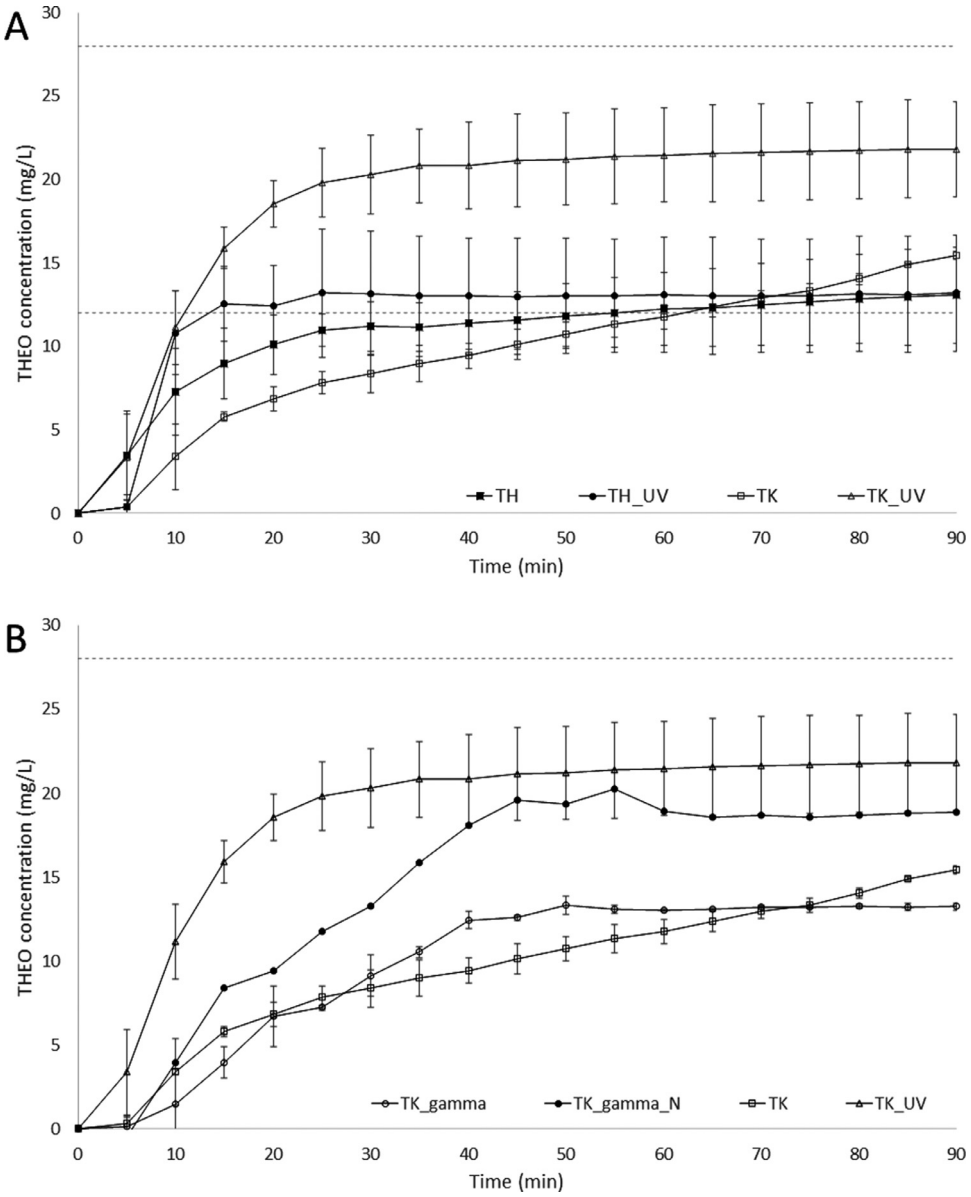

Fig. 4. The *in-vitro* theophylline (THEO) release of 3D-printed tablets. Fig. 4A: The dissolution of untreated and UV-crosslinked 3D-printed tablets (thin tablets TH_UV and thick tablets TK_UV). Fig. 4B: The dissolution of UV-crosslinked (TK_UV) and gamma-radiated (TK_gamma and TK_gamma_N) 3D-printed tablets. Standard deviations (n = 3, TK_gamma_N n = 1) and horizontal dashed lines for theoretical nominal concentrations are shown in both Fig. 4A and B.

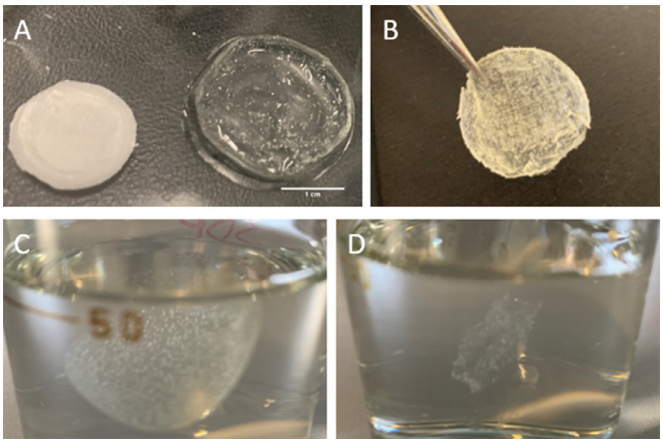

Fig. 5. Photographs of the 3D-printed tablets before, within and after a dissolution test *in vitro*. (A) Comparison of a thick UV-crosslinked (TK_UV) 3D-printed tablet before and after a dissolution test *in vitro* (scale bar equal to 1 cm); (B) The UV-crosslinked 3D-printed tablet (TK_UV) dried after a dissolution test *in vitro*; (C) The UV-crosslinked 3D-printed tablet after the exposition of 2 h to distilled water; (D) The UV-crosslinked solvent-cast free film after the exposition of 2 h to distilled water.

non-crosslinked thin and thick tablets were all completely dissolved by the end of the dissolution test. Our results are in agreement with those reported on the dissolution of Eudragit RL-based 3D-printed tablets presenting a prolonged THEO release behavior as the volume (*i.e.*, the number of layers) of the tablets was increased [47]. Since the drug release of 3D-printed tablets is dependent on a carrier polymer, this is important to be considered in adjusting ("tailoring") the individualized API dose and release pattern for the patients via the volume changes of 3D printed tablets.

Based on the visual inspection, the UV-crosslinked 3D-printed tablets presented an insoluble residue in the dissolution vessel after completing the dissolution test *in vitro* (90 min). We also found that the water uptake of such TH_UV and TK_UV tablets on the course of a dissolution test was on average 526% and 611%, respectively (Table 1B). The increase in weight, however, only shows swelling and does not consider the potential weight changes caused by either THEO dissolution or PEO dissolution/erosion. TK_UV tablets were enlarged in size, but the shape of the tablets did not change (Fig. 5A). When the tablets were dried, a characteristic crisscross pattern (surface texture) caused by the deposited material can be seen (Fig. 5B). Interestingly, when a solvent cast UV-crosslinked PEO films of equivalent diameter and thickness were dissolved in distilled water for a same time period as the 3D-printed tablets, the films lost their structure and shape (Fig. 5C). Further studies on the importance of material deposition itinerary could present more insight into this phenomenon.

These crosslinked extrusion-based 3D-printed tablets are the multilayer-structured systems with interlayer spaces. The importance of the porosity of PEO hot-melt extrudates in drug release has been discussed in the literature [48]. The porosity and subsequent drug release of traditional compressed tablets are dependent on the compression force, while the extrusion-based 3D-printed are composed of the deposited layers of semisolid material, which enables larger interlayer spaces. Crosslinking such 3D-printed tablets results in a loose tablet structure enabling the API to release and dissolve faster. With the non-crosslinked 3D-printed tablets, a viscous gel-layer is formed around the tablet, thus prolonging the drug release (THEO) from the tablet.

As seen in Fig. 4B, gamma-irradiated TK (thick) tablets presented a slow drug-release pattern similar to that obtained with the non-crosslinked TK tablets. The TK 3D-printed tablets kept in a nitrogen environment during gamma irradiation exhibited faster drug release similar to that observed with the UV-crosslinked TK tablets. As seen in Fig. 1B, the present two sets of 3D-printed tablets showed also the similar FTIR spectra. Nonetheless, the gamma-radiated 3D-printed tablets did not have any residue left to be weighed after a dissolution test.

4. Conclusions

The printability and behavior of a polymer solution in a 3D-printing process is largely dictated by the characteristics of a carrier polymer. PEO gel-like solutions enable the successful extrusion-based 3D-printing of layered THEO-loaded tablets. Both UV- and gamma-radiation (in a nitrogen environment) can be considered for crosslinking the PEO-based 3D-printed tablets. The drug release behavior of such 3D-printed tablets can be altered by both the addition of the number of polymeric layers and modifying crosslinking parameters. Moreover, the geometry of the 3D-printed tablets affects the drug release behavior. Further research work is needed on the effects of structure, porosity, and geometry of 3D-printed gel-forming tablets on the drug release to gain more thorough knowledge about the potential of such DDSs for a tailored drug delivery. The present printing formulations could also be improved by the addition of antioxidant to stabilize PEO as a carrier polymer. The effects of antioxidant on the drug release of the 3D-printed PEO-based DDSs need to be clarified.

Declaration of Competing Interests

The authors declare that they have no known competing financial interests or personal relationships that could have appeared to influence the work reported in this paper.

Acknowledgments

The present study is part of the Estonian national research projects (IUT34–18 and PRG726) funded by the Estonian Research Council and the Ministry of Education and Research, and the Nordic POP (patient-oriented products) project (a Nordic University Hub project #85352) funded by NordForsk.

References

[1] Goole J, Amighi K. 3D printing in pharmaceutics: a new tool for designing customized drug delivery systems. Int J Pharm 2016;499:376–94. doi: 10.1016/j.ijpharm.2015.12.071.
[2] Vaz VM, Kumar L. 3D Printing as a promising tool in personalized medicine. AAPS PharmSciTech 2021;22:49. doi: 10.1208/s12249-020-01905-8.
[3] Trenfield SJ, Awad A, Goyanes A, Gaisford S, Basit AW. 3D Printing Pharmaceuticals: drug Development to Frontline Care. Trends Pharmacol Sci 2018:1–12. doi: 10.1016/j.tips.2018.02.006.
[4] Azad MA, Olawuni D, Kimbell G, Badruddoza AZ, Hossain S, Sultana T. Polymers for extrusion-Based 3D printing of pharmaceuticals : a holistic materials – process perspective. Pharmaceutics 2020;12:124.
[5] Jacob S, Nair AB, Patel V, Shah J. 3D Printing Technologies : recent Development and Emerging Applications in Various Drug Delivery Systems. AAPS PharmSciTech 2020;21:220. doi: 10.1208/s12249-020-01771-4.
[6] Liravi F, Darleux R, Toyserkani E. Additive manufacturing of 3D structures with non-Newtonian highly viscous fluids : finite element modeling and experimental validation. Addit Manuf 2017;13:113–23. doi: 10.1016/j.addma.2016.10.008.
[7] Khaled SA, Alexander MR, Wildman RD, Wallace MJ, Sharpe S, Yoo J, et al. 3D extrusion printing of high drug loading immediate release paracetamol tablets. Int J Pharm 2018;538:223–30. doi: 10.1016/j.ijpharm.2018.01.024.
[8] El Aita I, Breitkreutz J, Quodbach J. Investigation of semi-solid formulations for 3D printing of drugs after prolonged storage to mimic real-life applications. Eur J Pharm Sci 2020;146:105266. doi: 10.1016/j.ejps.2020.105266.
[9] He Y, Yang F, Zhao H, Gao Q, Xia B, Fu J. Research on the printability of hydrogels in 3D bioprinting. Sci Rep 2016;6:1–13. doi: 10.1038/srep29977.
[10] Aguilar-de-Leyva Á, Linares V, Casas M, Caraballo I. 3D Printed Drug Delivery Systems Based on Natural Products. Pharmaceutics 2020;12:620.
[11] Kjar A, Huang Y. Application of Micro-Scale 3D Printing in Pharmaceutics. Pharmaceutics 2019;11:390.
[12] Cui M, Yang Y, Jia D, Li P, Li Q, Chen F, et al. Effect of novel internal structures on printability and drug release behavior of 3D printed tablets. J Drug Deliv Sci Technol 2019;49:14–23. doi: 10.1016/j.jddst.2018.10.037.

[13] Hoffman AS. Hydrogels for biomedical applications. Adv Drug Deliv Rev 2012;64:18–23. doi: 10.1016/j.addr.2012.09.010.
[14] Wang Y, Xi L, Zhang B, Zhu Q, Su F, Jelonek K, et al. Bioresorbable hydrogels prepared by photo-initiated crosslinking of diacrylated PTMC-PEG-PTMC triblock copolymers as potential carrier of antitumor drugs. Saudi Pharm J 2020;28:290–9. doi: 10.1016/j.jsps.2020.01.008.
[15] Uddin S, Ju J. Effect of crosslinking agents on drug distribution in chitosan hydrogel for targeted drug delivery to treat cancer. J Polym Res 2020:27.
[16] Galarraga JH, Kwon MY, Burdick JA. 3D bioprinting via an in situ crosslinking technique towards engineering cartilage tissue. Sci Rep 2019;9 19987. doi: 10.1038/s41598-019-56117-3.
[17] Sümbelli Y, Diltemiz SE, Say MG, Ünlüer ÖB, Erzös A, Say R. In situ and non-cytotoxic cross-linking strategy for 3D printable biomaterials. Soft Matter 2021;17:1008–15. doi: 10.1039/d0sm01734e.
[18] Robinson TM, Talebian S, Foroughi J, Yue Z, Fay CD, Wallace GG. Fabrication of Aligned Biomimetic Gellan Gum-Chitosan Microstructures through 3D Printed Microfluidic Channels and Multiple In Situ Cross-Linking Mechanisms. ACS Biomater Sci Eng 2020;6:3638–48. doi: 10.1021/acsbiomaterials.0c00260.
[19] Tang C, Saquing CD, Harding JR, Khan SA. In situ cross-linking of electrospun poly (vinyl alcohol) nanofibers. Macromolecules 2010;43:630–7. doi: 10.1021/ma902269p.
[20] Stone SA, Gosavi P, Athauda TJ, Ozer RR. In situ citric acid crosslinking of alginate /polyvinyl alcohol electrospun nanofibers. Mater Lett 2013;112:32–5. doi: 10.1016/j.matlet.2013.08.100.
[21] J. Herzberger, K. Niederer, H. Pohlit, J. Seiwert, M. Worm, F.R. Wurm, H. Frey, Polymerization of Ethylene Oxide, Propylene Oxide, and Other Alkylene Oxides: synthesis, Novel Polymer Architectures, and Bioconjugation, (2015). doi:10.1021/acs.chemrev.5b00441.
[22] Viidik L, Seera D, Antikainen O, Kogermann K, Heinämäki J, Laidmäe I. 3D-printability of aqueous poly (ethylene oxide) gels. Eur Polym J 2019;120:109206. doi: 10.1016/j.eurpolymj.2019.08.033.
[23] Isreb A, Baj K, Wojsz M, Isreb M, Peak M. 3D printed oral theophylline doses with innovative 'radiator-like' design : impact of polyethylene oxide (PEO) molecular weight. Int J Pharm 2019;564:98–105. doi: 10.1016/j.ijpharm.2019.04.017.
[24] Fina F, Goyanes A, Madla CM, Awad A, Tren SJ. 3D printing of drug-loaded gyroid lattices using selective laser sintering. Int J Pharm 2018;547:44–52. doi: 10.1016/j.ijpharm.2018.05.044.
[25] Doytcheva M, Dotcheva D, Stamenova R, Tsvetanov C, Polyox NK, P.N.- K. UV-Initiated Crosslinking of Poly (ethylene oxide) with Pentaerythritol Triacrylate in Solid State. Macromol Mater Eng 2001;286:30–3.
[26] Zhou C, Wang Q, Wu Q. UV-initiated crosslinking of electrospun poly (ethylene oxide) nanofibers with pentaerythritol triacrylate : effect of irradiation time and incorporated cellulose nanocrystals. Carbohydr Polym 2012;87:1779–86. doi: 10.1016/j.carbpol.2011.09.095.
[27] Wong RSH, Ashton M, Dodou K. Effect of Crosslinking Agent Concentration on the Properties of Unmedicated Hydrogels. Pharmaceutics 2015;7:305–19. doi: 10.3390/pharmaceutics7030305.
[28] Kronfli E, Lovell KV, Hooper A, Neat RJ. The Conductivity Behaviour of Gammairradiated PEO-LiX Electrolytes. I, Br Polym J 1988;20:275–80.
[29] Ferloni P, Magistris A, Chiodelli G, Faucitano A, Buttafava A. Effects of gamma-radiation on electrolytes: PEO and PEO2o-LiC104. Radiat Phys Chem 1991;37:615–21.
[30] Pucić I, Turković A. Radiation modification of (PEO)8ZnCl2 polyelectrolyte and nanocomposite. Solid State Ionics 2005;176:1797–800. doi: 10.1016/j.ssi.2005.04.042.
[31] Jurkin T, Pucić I. Poly (ethylene oxide) irradiated in the solid state, melt and aqueous solution — a DSC and WAXD study. Radiat Phys Chem 2012;81:1303–8. doi: 10.1016/j.radphyschem.2011.12.021.
[32] Maitra J, Shukla VK. Cross-linking in Hydrogels - a Review. Am J Polym Sci 2014;4:25–31. doi: 10.5923/j.ajps.20140402.01.
[33] Song X, Dong P, Gravesande J, Cheng B, Xing J. UV-mediated solid-state cross-linking of electrospinning nano fibers of modified collagen. Int J Biol Macromol 2018;120:2086–93. doi: 10.1016/j.ijbiomac.2018.09.029.
[34] Cilurzo F, Selmin F, Minghetti P, Adami M, Bertoni E, Lauria S, et al. Injectability Evaluation : an Open Issue. AAPS PharmSciTech 2011;12:604–9. doi: 10.1208/s12249-011-9625-y.
[35] Meruva S, Donovan MD. Polyethylene Oxide (PEO) Molecular Weight Effects on Abuse-Deterrent Properties of Matrix Tablets. AAPS PharmSciTech 2020;21:28. doi: 10.1208/s12249-019-1565-y.
[36] Noor SAM, Ahmad A, Talib IA, Rahman MYA. Effect of ZnO nanoparticles filler concentration on the properties of PEO-ENR50-LiCF 3 SO 3 solid polymeric electrolyte. Ionics (Kiel) 2011:451–6. doi: 10.1007/s11581-011-0534-6.
[37] Nokhodchi A, Okwudarue ON, Valizadeh H, Momin MN. Cogrinding as a Tool to Produce Sustained Release Behavior for Theophylline Particles Containing Magnesium Stearate. AAPS PharmSciTech 2009;10. doi: 10.1208/s12249-009-9326-y.
[38] Lin H, Hsu P, Lin S. Theophylline e citric acid co-crystals easily induced by DSC e FTIR microspectroscopy or different storage conditions. Asian J Pharm Sci 2013;8:19–27. doi: 10.1016/j.ajps.2013.07.003.
[39] Hakkarainen E, Kõrkjas A, Laidmäe I, Lust A, Semjonov K, Kogermann K, et al. Comparison of traditional and ultrasound-enhanced electrospinning in fabricating nanofibrous drug delivery systems. Pharmaceutics 2019;11:495.
[40] Hennink WE, Van Nostrum CF. Novel crosslinking methods to design hydrogels. Adv Drug Deliv Rev 2002;54:13–36. doi: 10.1016/j.addr.2012.09.009.
[41] Teixeira RSP, Correa RJ, Belvino A, Nascimento RSV. UV Irradiation-Induced Crosslinking of Aqueous Solution of Poly (ethylene oxide) with Benzophenone as Initiator. J Appl Polym Sci 2013;130:2458–67. doi: 10.1002/app.39381.
[42] Crowley MM, Zhang F, Koleng JJ, McGinity JW. Stability of polyethylene oxide in matrix tablets prepared by hot-melt extrusion. Biomaterials 2002;23:4241–8.
[43] Van Renterghem J, Vervaet C, De Beer T. Rheological characterization of molten polymer-drug dispersions as a predictive tool for pharmaceutical hot-melt extrusion processability. Pharm Res 2017;34:2312–21. doi: 10.1007/s11095-017-2239-7.
[44] El Aita I, Breitkreutz J, Quodbach J. On-demand manufacturing of immediate release levetiracetam tablets using pressure-assisted microsyringe printing. Eur J Pharm Biopharm 2019;134:29–36. doi: 10.1016/j.ejpb.2018.11.008.
[45] Clevers JGPW, Kooistra L, Schaepman ME. Using spectral information from the NIR water absorption features for the retrieval of canopy water content. Int J Appl Earth Obs Geoinf 2008;10:388–97. doi: 10.1016/j.jag.2008.03.003.
[46] Giangiacomo R. Study of water – sugar interactions at increasing sugar concentration by NIR spectroscopy. Food Chem 2006;96:371–9. doi: 10.1016/j.foodchem.2005.02.051.
[47] Pietrzak K, Isreb A, Alhnan MA. A flexible-dose dispenser for immediate and extended release 3D printed tablets. Eur J Pharm Biopharm 2015;96:380–7. doi: 10.1016/j.ejpb.2015.07.027.
[48] Cantin O, Siepmann F, Willart JF, Danede F, Siepmann J, Karrout Y. PEO hot melt extrudates for controlled drug delivery : importance of the type of drug and loading. J Drug Deliv Sci Technol 2021;61:102238. doi: 10.1016/j.jddst.2020.102238.